



RESEARCH ARTICLE

10.1002/2013GC005113

A 249 kyr stack of eight loess grain size records from northern China documenting millennial-scale climate variability

Shiling Yang and Zhongli Ding

Key Laboratory of Cenozoic Geology and Environment, Institute of Geology and Geophysics, Chinese Academy of Sciences, Beijing, China

Key Points:

- A 249 kyr loess grain size stack documents millennial-scale climate variability
- Atmospheric forcing mechanisms control millennial-scale signal transmission
- The climate of northern China during MIS 7d was similar to that of MIS 6

Supporting Information:

- Readme for Auxiliary Material
- Table S1

Correspondence to:

S. Yang,
yangsl@mail.iggcas.ac.cn

Citation:

Yang, S., and Z. Ding (2014), A 249 kyr stack of eight loess grain size records from northern China documenting millennial-scale climate variability, *Geochem. Geophys. Geosyst.*, 15, 798–814, doi:10.1002/2013GC005113.

Received 24 OCT 2013

Accepted 27 JAN 2014

Accepted article online 5 FEB 2014

Published online 31 MAR 2014

Abstract In order to construct a stacked climatic record of millennial-scale variability for northern China, grain size was measured for 12,330 samples from eight thick loess sections. Between section correlation of these grain size records shows that, although small depositional hiatuses may be present within a single section, most parts of the sections display continuous dust deposition. By correlating the eight records with the precisely dated Chinese stalagmite $\delta^{18}\text{O}$ record, a stacked 249 kyr-long grain size time series was constructed, termed the “CHILOMOS” record, which is the first high-resolution stack documenting millennial-scale variability in northern China. This stack shows millennial-scale climatic events superimposed on a prominent cooling trend during the last and penultimate glaciations, consistent with the pattern of increasing global ice volume. However, this cooling trend is dampened in the stalagmite record and totally suppressed in the low-latitude ocean record. It follows that the Loess Plateau, far from the low-latitude ocean, is largely influenced by the northern high-latitude ice sheets, while the proximal stalagmites of southern China primarily document signals from the low-latitude ocean. Cross correlations of climatic records from high and low latitudes demonstrate that the millennial-scale abrupt changes originated in the northern polar area and were propagated into East Asia largely through the East Asian winter monsoon. The CHILOMOS record also confirms that the driest and coldest interval of the last 249 kyr occurred in the late MIS 6, and that MIS 7d was extremely cold and dry, similar to the stadial conditions of MIS 6.

1. Introduction

Numerous studies have shown that the climate system underwent rapid fluctuations on a millennial time scale during the last glaciation [e.g., Dansgaard *et al.*, 1993; Grootes *et al.*, 1993; Voelker and Workshop Participants, 2002; Clement and Peterson, 2008]. High-resolution oxygen-isotope records from Greenland ice cores have demonstrated that abrupt temperature changes of up to 16°C [Lang *et al.*, 1999; Landais *et al.*, 2004; Huber *et al.*, 2006], known as Dansgaard-Oeschger (D-O) events, occurred during the last glaciation [Dansgaard *et al.*, 1993; Grootes *et al.*, 1993]. A series of rapid temperature oscillations closely matching those in the ice-core record are also documented in North Atlantic sediments [Bond *et al.*, 1993]. These oscillations can be bundled into longer cooling cycles (Bond cycles) with asymmetrical saw-tooth shapes [Bond *et al.*, 1993]. Each Bond cycle is defined by a succession of progressively cooler interstadials, culminating in an enormous discharge of icebergs into the North Atlantic (a Heinrich (H) event [Heinrich, 1988]), followed by an abrupt shift to a warmer climate over several decades [Bond *et al.*, 1993].

Stimulated by studies of ice cores and deep sea sediments, millennial-scale events have been identified from different sediments worldwide [Voelker and Workshop Participants, 2002]. East Asia has received much attention in this regard, as the East Asian monsoon system is crucial in the latitudinal transfer of heat and moisture between the tropics and high latitudes [Chen *et al.*, 1991; Webster *et al.*, 1998; Wang *et al.*, 2003]. Remarkable records have been derived from the stalagmites of southern China, with high resolution, millennial-scale climate variability having been well established for the past two glacial-interglacial cycles [Cheng *et al.*, 2006; Wang *et al.*, 2008]. In the past two decades, researchers have identified most of the D-O cycles and Heinrich events from the last glacial loess deposits in northern China [Porter and An, 1995; Chen *et al.*, 1997; Ding *et al.*, 1998; Fang *et al.*, 1999; Sun *et al.*, 2012]. However, the millennial-scale oscillations for earlier glacial periods are poorly understood, although the climatic instability of earlier glaciations on the Loess Plateau has been recognized [Ding *et al.*, 1999; Lu *et al.*, 1999]. Furthermore, it remains unclear whether millennial-scale events in northern China are similar to those in the south in pattern, structure, and strength.

Loess deposits with high-sedimentation rates, commonly found in the northern Loess Plateau due to its proximity to the dust source area, are valuable archives of millennial-scale climate variability [Chen *et al.*, 1997; Ding *et al.*, 1998, 1999]. Recently, some studies [Stevens *et al.*, 2006] cast doubt upon the continuity of loess deposition based on the results of optically stimulated luminescence (OSL) dating, whereas others have supported the continuity based on OSL dating [Lu *et al.*, 2007; Sun *et al.*, 2012] and geomagnetic excursion studies [Zhu *et al.*, 2007]. As a terrestrial sediment type, hiatuses of varying magnitude might well be expected during the accumulation of subaerial dust due to locally varying factors such as topographic and geomorphologic conditions, the configuration of the loess-desert distribution, and wind trajectories [Liu, 1985; Yang and Ding, 2004, 2008]. Thus, it is possible that dust deposits in a single section may have poor continuity within some time intervals. However, loess depositional hiatuses are unlikely to be synchronous over a sufficiently large depositional area, and therefore a comprehensive analysis of records from different sites would ensure that millennial-scale events will mostly be recorded in the loess.

In loess-paleosol sequences, paleosols are consistently characterized by finer particle sizes than the loess horizons above and below them. The change in grain size was thought in earlier studies to reflect the intensity of winter monsoon winds that transported the loess grains [An *et al.*, 1991; Ding *et al.*, 1994; Xiao *et al.*, 1995], thereby suggesting a considerable increase in the intensity of the winter monsoon during glacial periods. However, recent studies have shown that temporal-spatial grain size changes in Chinese loess on orbital time scales are principally controlled by the source-to-sink distance [Yang and Ding, 2004, 2008; Ding *et al.*, 2005]. Since the desert margin environment is very sensitive to changes in summer monsoon rainfall, the loess grain size can thus be regarded as a proxy for summer monsoon changes [Yang and Ding, 2008]. On millennial time scales, however, it is possible that winter monsoon velocity changes may affect loess grain size. In practice, an increase in winter monsoon velocity and a decrease in summer monsoon rainfall would both occur within the same time intervals. Thus, grain size can reliably be used as a proxy for aridity changes, with coarse particle sizes indicating cold and dry climate conditions, and vice versa.

A stacked 2.6 Myr grain size record for Chinese loess was previously developed based on five sections from the central and southern Loess Plateau [Ding *et al.*, 2002]. This record displays obvious climatic events on orbital time scales, but those on millennial scales were subdued due to low dust sedimentation rates in the south. In the northern Loess Plateau, the dust sedimentation rates are 2–3 times higher than in the southern part, so the dust deposits in the north have the potential to document more detailed climatic signals. However, a comprehensive climatic record with a temporal resolution higher than orbital time scales remains to be developed, despite the fact that several high-resolution loess sections from the northern plateau have been reported [e.g., Chen *et al.*, 1997; Ding *et al.*, 1998, 1999].

In this study, eight high-resolution grain size records were generated from eight loess sections located in different places on the Loess Plateau. Intersectional correlation of the grain size records allows the recognition of small depositional hiatuses within a single loess sequence, and the identification of most of the millennial-scale climatic events for the past two glacial cycles. The time scale for each section was developed through correlation with precisely dated stalagmite records [Wang *et al.*, 2008; Cheng *et al.*, 2012]. The time scales thus obtained for each section were then used to generate a stacked grain size time series for the past 249 kyr, with the aim of exploring the mechanisms linking millennial-scale climate variability in the Loess Plateau to that in the northern polar area.

2. Setting and Stratigraphy

Eight loess sections in the northern Loess Plateau, located from west to east at Linxia (35.62°N, 103.20°E), Xinzhuangyuan (36.19°N, 104.73°E), Lijiayuan (36.12°N, 104.86°E), Hongde (36.77°N, 107.21°E), Huanxian (36.65°N, 107.26°E), Jiyuan (37.14°N, 107.39°E), Huachi (36.34°N, 107.93°E), and Zichang (37.14°N, 109.85°E) (Figure 1), were logged and sampled. At present, there is a positive eastward gradient in both mean annual temperature (from ~7 to ~9°C) and mean annual precipitation (from ~250 to ~500 mm) for these sites. Most sections consist of the loess (L)-soil (S) sequence S0, L1, S1, L2, and S2 (Figure 2). In the Zichang section, S0 has been eroded completely, while only the S0-L1-S1 sequence was found in the Jiyuan and Linxia sections.

The Holocene soil S0 is characterized by a massive structure, a relative abundance of dark organic matter, and a few white-colored secondary carbonate pseudomycelia. The loess units L1 and L2 were deposited

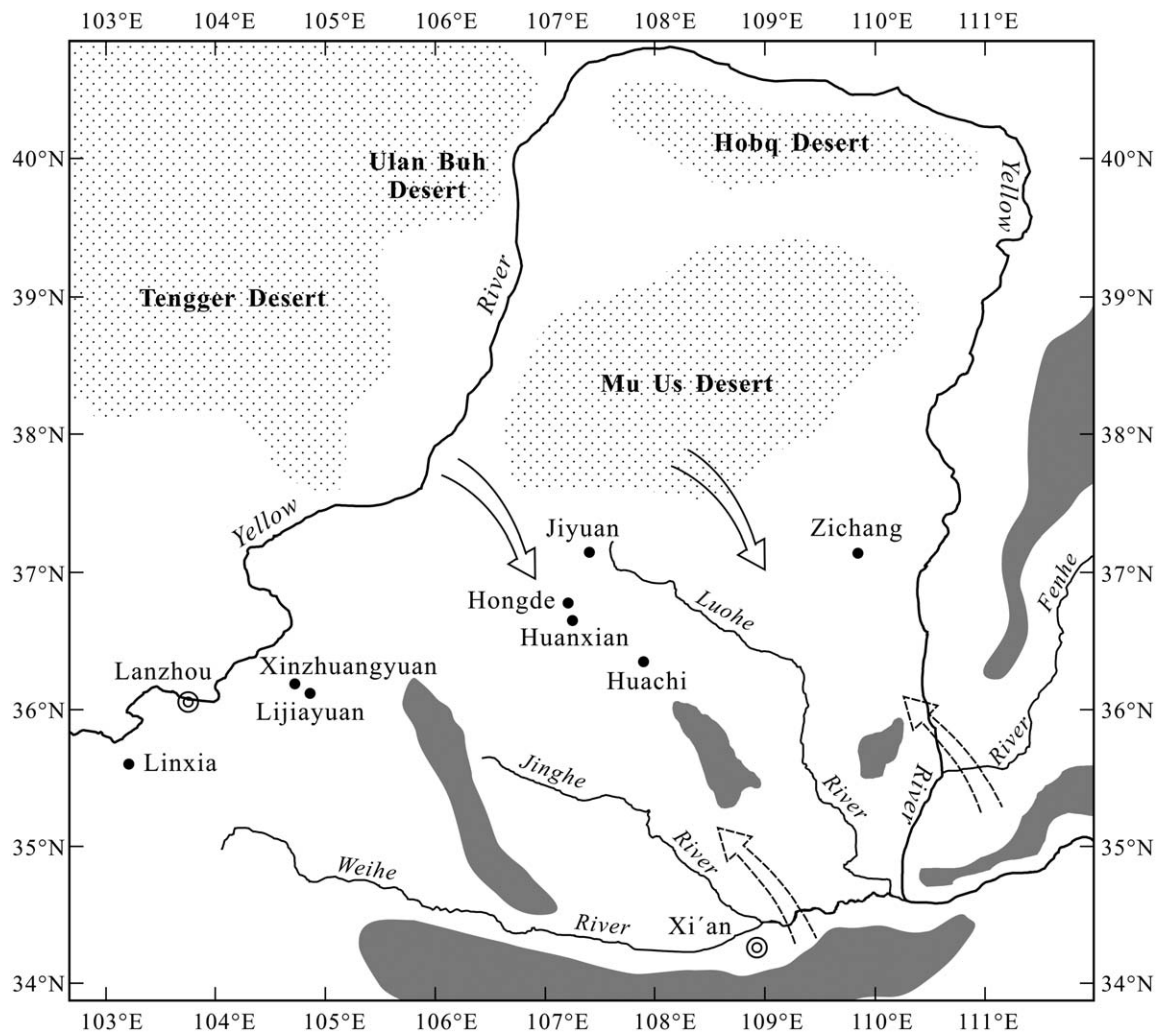


Figure 1. Map showing the study sites (solid circles) in the Chinese Loess Plateau. The deserts (dotted) to the north of the Loess Plateau and the mountains (shaded) along and within the Loess Plateau are also indicated. The solid and dashed arrows indicate the East Asian winter and summer monsoon winds, respectively.

during the last and penultimate glacial periods, respectively. Both L1 and L2 are yellowish in color and massive in structure, ranging in thickness from 17 to 30 m. The L1 loess unit can generally be divided into five subunits, L1-1, L1-2, L1-3, L1-4, and L1-5 (Figure 2). L1-2 and L1-4 are weakly developed soils, and the others are typical loess horizons. Previous authors [Kukla, 1987; Lu *et al.*, 2007; Ding *et al.*, 2002] have shown that L1-1 is correlated with marine isotope stage (MIS) 2, L1-5 with MIS 4, and L1-2, L1-3, and L1-4 together with MIS 3. The fivefold subdivision of L1 is clearly expressed in the grain size curves shown in Figure 2. The L2 loess unit is also composed of three typical loess layers (L2-1, L2-3, and L2-5) and two weakly developed soils (L2-2 and L2-4), as suggested by the grain size curves (Figure 2). The L2 loess unit is correlated with MIS 6. The soil units S1 and S2, with thicknesses of 3–11 m, developed in the last and penultimate interglacial periods and are correlated with MIS 5 and 7, respectively [Kukla, 1987; Lu *et al.*, 2007; Ding *et al.*, 2002]. Both are brownish or reddish in color and have an A-Bw-C or A-Bt-C horizon sequence. The soil unit S1 consists of three individual soils (S1-1, S1-3, and S1-5) and two intervening loess beds (S1-2 and S1-4), which is particularly evident in the sections in the western loess plateau (e.g., Linxia, Xinzhuangyuan, and Lijiayuan). The soil unit S2 is composed of two soils (S2-1 and S2-2) and a thin intervening loess horizon.

A total of 12,330 samples were collected at 2–5 cm intervals. This sample spacing yields a mean depositional resolution of 50–250 years. Grain size was measured for all samples with a SALD-3001 laser diffraction particle analyzer. Ultrasonic pretreatment with addition of a 20% solution of $(\text{NaPO}_3)_6$ was used to disperse

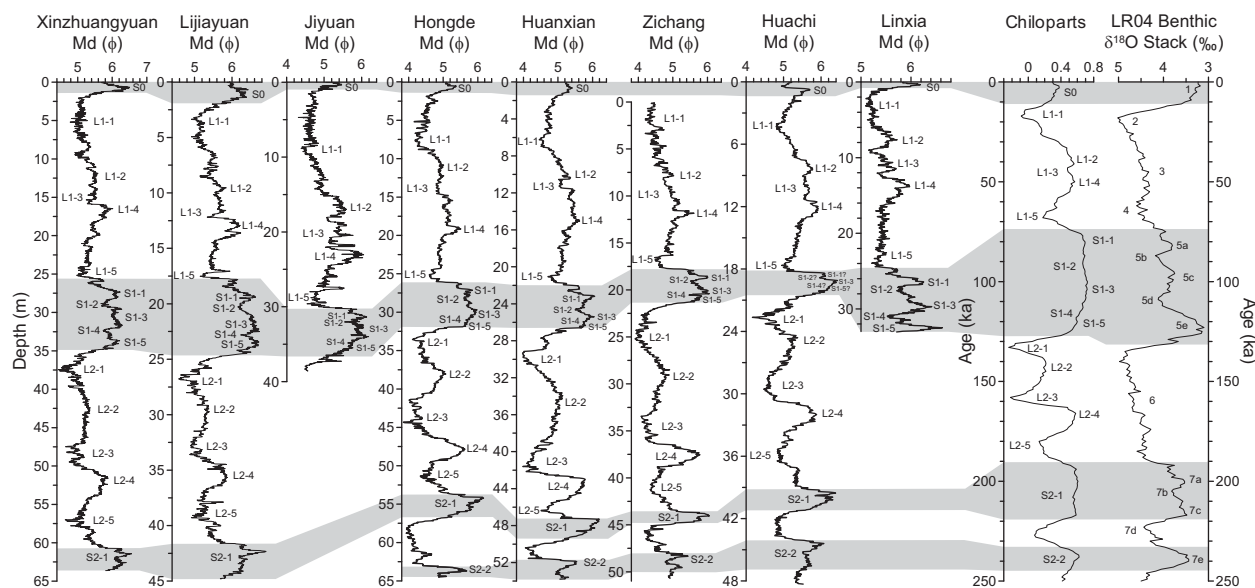


Figure 2. Median grain size (Md, phi scale) records for the eight loess sections, and correlation with a stacked benthic $\delta^{18}\text{O}$ record [Lisiecki and Raymo, 2005] and a stacked Chinese loess particle size record (Chiloparts) [Ding et al., 2002]. The shaded zones indicate interglacials. Subdivision of the loess-soil sequences is indicated. The depositional hiatuses and discrepancies suggested by intersite correlation of the grain size records are marked with "?". Interglacial paleosols (S0, S1, and S2), as well as weakly developed interstadial soils (L1-2, L1-4, L2-2, and L2-4), are consistently characterized by finer particle sizes than the loess horizons above and below them. Note that the depth scale varies from one section to another.

the samples prior to particle size determination [for details see Ding et al., 1999]. Repeat analyses show that this procedure yields an error of less than 0.6% for the median grain size (phi units).

3. Age Model

In previous studies, the time scales of millennial climate oscillations for Chinese loess were based mainly on the methods of thermoluminescence (TL) [Porter and An, 1995; Chen et al., 1997], OSL [Sun et al., 2012], and astronomical tuning [Ding et al., 1998]. Although such time scales are loosely constrained, they do enable us to ascertain which millennial-scale events are documented within a specific loess subunit (Table 1). As mentioned earlier, the loess subunits are clearly expressed in the structure of the grain size curves (Figure 2), i.e., the peak-trough alternations, and there is a great similarity in the structure of the grain size curve between the different loess sections. Based on these characteristics and previous correlations of loess records with the stalagmite and Greenland ice records [Chen et al., 1997; Ding et al., 1998; Cheng et al., 2012; Sun et al., 2012], the millennial-scale events can readily be recognized in each section (Figures 3 and 4), with grain size peaks indicating interstadials and troughs reflecting stadials. In this step, only the grain size oscillations with relative amplitudes larger than 1.2% (twice the analytical error) were designated as millennial-scale events. These events are herein named Chinese Loess Interstadials (CLIS) and the nomenclature of millennial-scale events used in Chinese stalagmites is adopted for them [Cheng et al., 2006; Wang et al., 2008], with the last glacial period CLIS being denoted CLIS A1, A2, and so on, from youngest to oldest, and those of the penultimate glacial period being denoted CLIS B1, B2, and so on (Table 1; Figures 3 and 4).

Grain size variability is very similar from one section to another; therefore, a cycle-to-cycle grain size correlation can practically be made (Figures 3 and 4). However, small discrepancies are present in four aspects. (1) Some millennial-scale events within a specific section are not as prominent as in other records, including the Younger Dryas (YD), the A1, A7, A9, and B5 events at Xinzhuangyuan, the B8 and B10 events at Lijiyuan, the A15, A17, B10, B11, B15, and B17 events at Hongde, the H2, A3, A5, A11, and B14 events at Huanxian, the A15 event at Zichang, and the A3, A9, A15, A19, and A20 events and a portion of A21-A22 at Huachi. (2) Some portions at a specific site are exceptionally thin compared to their counterparts in other sections, such as the A2-A3 portion at Hongde, the A10 event at Zichang, and the H1-H2 and S1-S portions at Huachi. (3) At Linxia, the A15 event and the grain size trough between A7 and A8 are evidently lacking,

Table 1. Time Duration of the Loess Subunits Together With Their Corresponding Marine Isotope Stages (MIS) and the Assigned Millennial-Scale Events^a

MIS	Loess Subunit	Orbital Age (ka)	Refined Age (ka)	Millennial-Scale Events Contained Within
2	L1-1	27–11	27–11	YD, A1, H1, A2, and H2
3	L1-2	42–27	38–27	A3–A8 and H3
3	L1-3	47–42	49–38	A9–A12, H4, and H5
3	L1-4	58–47	59–49	A13–A17
4	L1-5	73–58	73–59	H6, A18, and A19
5a	S1-1	85–73	91–73	A20–A22
5b	S1-2	94–85	99–91	
5c	S1-3	109–94	113–99	A23 and A24
5d	S1-4	114–109	118–113	
5e	S1-5	128–114	129–118	
6	L2-1	136–128	139–129	H11, B1, and B2
6	L2-2	155–136	160–139	B3–B12
6	L2-3	162–155	165–160	B13
6	L2-4	177–162	178–165	B14–B17
6	L2-5	190–177	192–178	B18 and B19
7a–c	S2-1	219–190	224–192	B20–B24
7d	Loess unit between S2-1 and S2-2	234–219	237–224	
7e	S2-2	245–234	247–237	

^aOrbital tuning ages for each loess unit are from the orbital time scales of Chinese loess [Ding et al., 1998, 2002], while the refined ages are based on correlation with precisely dated stalagmites [Cheng et al., 2012]. The nomenclature for Chinese interstadial events, i.e., “A” and “B” for the last and penultimate glacial period, respectively, follows Cheng et al. [2006] and Wang et al. [2008].

and the overlying A3–A7 part is relatively thin. (4) As a result of overall low dust accumulation rates in interglacials, some events appear to merge in the loess grain size records, such as the A21 and A22 events at Zichang, the A24 and A25 events at all the sites except Linxia, and the B20, B21, and B22 events in all the

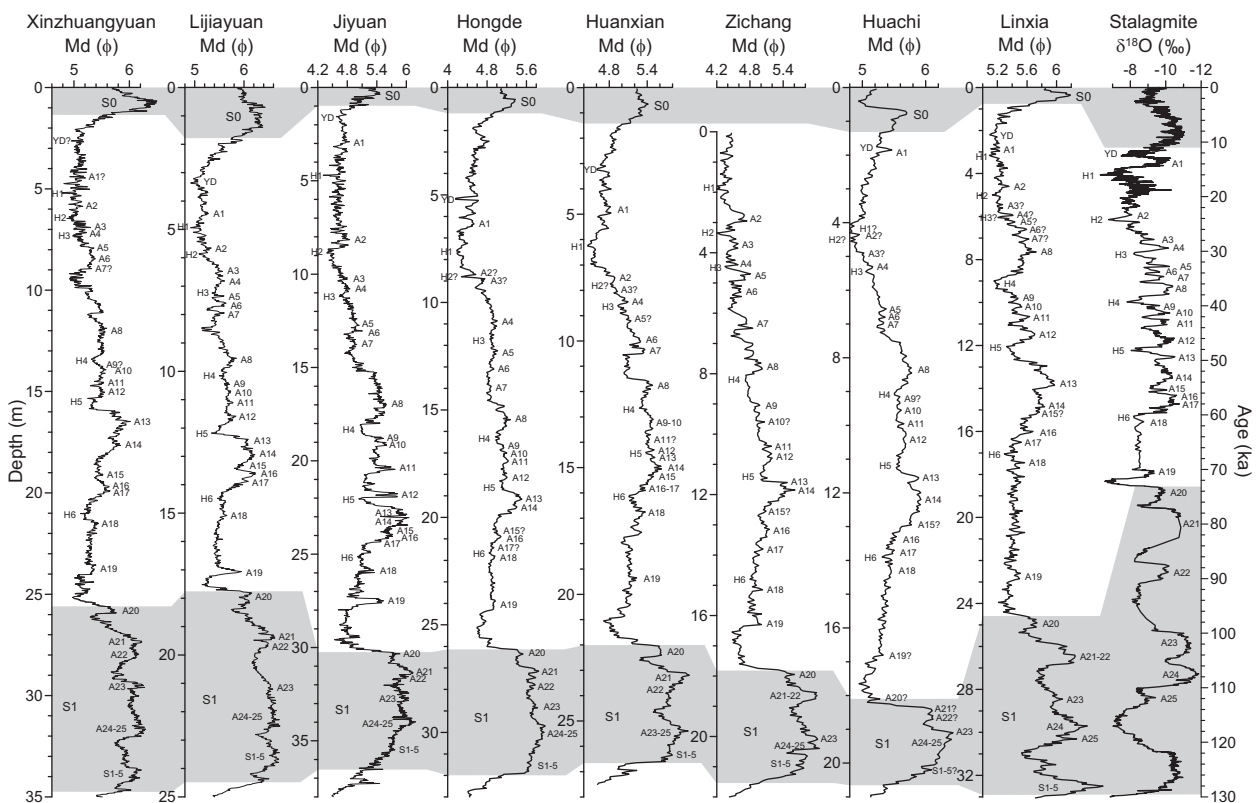


Figure 3. Median grain size (Md, phi scale) records of the eight loess sections above the S1 soil unit, and correlation with the stalagmite $\delta^{18}\text{O}$ record [Wang et al., 2008; Cheng et al., 2012]. The Chinese Loess Interstadial (CLIS) events (A1–A25) are identified in the loess grain size records for the last glacial-interglacial cycle, following the nomenclature used in the stalagmite record [Cheng et al., 2006; Wang et al., 2008]. The Younger Dryas (YD) and Heinrich (H) events are also identified in the grain size records. The millennial-scale events possibly disturbed by depositional hiatuses are marked with “?” and were excluded from the construction of the stacked grain size record shown in Figures 7–9.

sections. Even so, the merged B20–22 events are still not obvious at Hongde, Huanxian, and Zichang, suggesting the presence of small depositional hiatuses. Obviously, any substantial depositional hiatus can be detected by grain size correlation, which makes possible the reconstruction of an essentially complete sequence of millennial-scale climatic events using the grain size records.

The Chinese stalagmite $\delta^{18}\text{O}$ records are excellent archives of East Asian monsoon climate variability, documenting all the millennial climate oscillations recorded in Greenland [Wang *et al.*, 2001, 2008]. Since loess chronological studies cannot provide accurate age constraints, the stalagmite record can be directly used as a standard to refine the Chinese loess time scale, which also records monsoon variability. The identified millennial-scale events in the loess records (Table 1; Figures 3 and 4) were tied to the corresponding ones in the stalagmite $\delta^{18}\text{O}$ record. Taking the ages of these events from the stalagmite record [Cheng *et al.*, 2012] as time controls and then using linear interpolation, a refined time scale for each of the grain size records was established. In so doing, only small age adjustments were needed from the orbital tuning ages [Ding *et al.*, 2002] for most of the events (Table 1). In this procedure, both the synchronicity of the summer monsoon between southern and northern China and a constant sedimentation rate between age-depth control points were assumed.

4. Stacked Grain Size Record

To stack a representative grain size record from the sections, it is crucial to determine which parts of a single record should be excluded. By correlating the grain size records between sections, small depositional hiatuses and cases of inconsistent grain size variability were identified (Figures 3–6), and were excluded from the construction of the stacked grain size record. In addition, the 3.5 m thick uppermost part of L1 in the Zichang section (the H1–H2 portion) was left out, because of the possible erosional effect due to the absence of the overlying S0 (Figures 3 and 5). The eight grain size records were stacked together according to the following procedures. First, each grain size time series was interpolated linearly at 200 year intervals (Figures 5 and 6). Then, each was normalized in order to give the same weighting to all records in the stack. Finally, the grain size data at each time level were averaged to form a new time series (Figures 7–9), for which the acronym “CHILOMOS” (Chinese Loess Millennial-scale Oscillation Stack) is herein proposed. The CHILOMOS data are presented in supporting information Table S1.

4.1. Millennial-Scale Oscillations for the Last Glaciation

The Greenland interstadials 1–19 (D-O 1–19) are well documented in the last glacial loess unit (L1) in northern China (Figure 7). Most of the long-lasting D-O events in Greenland, e.g., D-O 8, 12, and 14, are also evident in the Loess Plateau, as well as in the South China Sea and Antarctica. Similarly, the short-duration D-O events in Greenland, such as D-O 2–7, 9, 15, and 18, have their damped counterparts in the Loess Plateau, the South China Sea, and Antarctica. However, there are evident differences in the details between the grain size and Greenland $\delta^{18}\text{O}$ records. First, the Greenland ice record shows large-amplitude oscillations, while the loess grain size record displays relatively small oscillations. Second, the D-O cycles are superimposed on a gradual coarsening trend in grain size from ~ 50 to ~ 25 ka, while they show a somewhat stable oscillation in Greenland during the whole of the last glaciation. Finally, some prominent cold events in Greenland are not as evident in the Loess Plateau, such as the YD, H3, and H6 events.

The loess grain size record has more similarities with the stalagmite $\delta^{18}\text{O}$ record than the ice-core record (Figure 7). For example, the long-duration A8, A12, and A14 events and the stadial between A19 and A20 are prominent in the stalagmite record, and their counterparts in the Chinese loess record are also evident. Furthermore, the A3, A9, A15, and A18 events are weak in both the stalagmite and loess records. The most striking discrepancy between the two records is that the D-O events in MIS 3 are superimposed on a gradual coarsening trend in the loess record, whereas this phenomenon is not seen in the stalagmite record.

4.2. Millennial-Scale Oscillations for the Penultimate Glaciation

For this time interval, all the millennial-scale events except B13 show close agreement between the loess and stalagmite records (Figure 8), as shown by the similar oscillation pattern of the two curves. Among the events, B15, B16, and B17 appear to be exceptionally warm, humid interstadials and H11 is the coldest and driest interval, all being clearly reflected in both the loess and stalagmite records. The Antarctic ice record shows large-amplitude temperature oscillations in the interval containing the B12–B19 events, generally

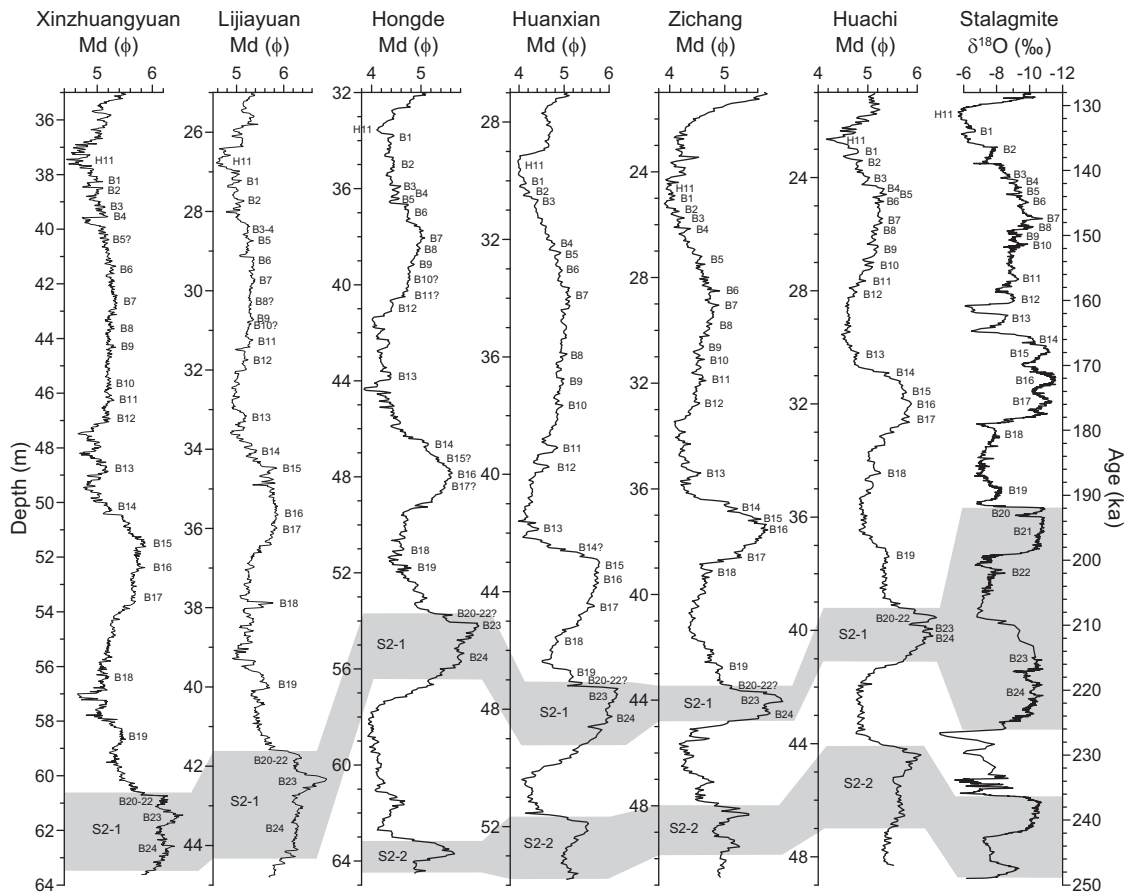


Figure 4. Median grain size (Md, phi scale) records for the S2-L2 portion of the loess sections at Xinzhuangyuan, Lijiyuan, Hongde, Huanxian, Zichang, and Huachi, and correlation with the stalagmite $\delta^{18}\text{O}$ record [Wang *et al.*, 2008; Cheng *et al.*, 2012]. The Chinese Loess Interstadial (CLIS) events (B1–B24) are identified in the loess grain size records for the penultimate glacial-interglacial cycle, following the nomenclature used in the stalagmite record [Cheng *et al.*, 2006; Wang *et al.*, 2008]. The millennial-scale events possibly disturbed by depositional hiatuses are marked with “?” and were excluded from the construction of the stacked grain size record shown in Figures 8 and 9.

consistent with the stalagmite and loess records (Figure 8). In addition, from the early to the late MIS 6, the loess grain size record shows a pronounced gradual coarsening trend, while only a slight positive shift in the stalagmite $\delta^{18}\text{O}$ is observed.

4.3. Millennial-Scale and Orbital-Scale Oscillations for the Last and Penultimate Interglacial Complexes

The Greenland ice core and stalagmite $\delta^{18}\text{O}$ records show large-amplitude oscillations for MIS 5 and 7 (Figure 9), similar to those of glacial periods. In contrast, the stacked grain size record exhibits relatively small-amplitude oscillations for the two interglacials. Some millennial-scale events are even partially or completely merged, such as A21–A22, A24–A25, and B20–B22, probably as a result of low dust sedimentation rates and relatively stable climatic conditions in the interglacial Loess Plateau [Chen *et al.*, 1999; Ding *et al.*, 1999].

In addition, MIS 7d is characterized by a grain size trough nearly as prominent as those of the stadials in MIS 6 (Figure 9). The present results and previous studies [Yang and Ding, 2008] confirm that the driest and coldest intervals of the last two glacial periods occurred in MIS 6, as indicated by the H11 event and the stadials preceding and following the B13 event. The CHILOMOS record thus implies that MIS 7d was dominated by extremely cold, dry climate conditions, similar to the stadial conditions of MIS 6. This is also evident in the stalagmite and benthic $\delta^{18}\text{O}$ records, as well as in the Antarctic temperature record (Figure 9). Furthermore, records from the North Atlantic [e.g., Ruddiman and McIntyre, 1982; Roucoux *et al.*, 2006; Penaud *et al.*, 2008], Europe [e.g., Tzedakis *et al.*, 2003; Roucoux *et al.*, 2008], and Siberia [Prokopenko *et al.*, 2001] all show MIS 7d

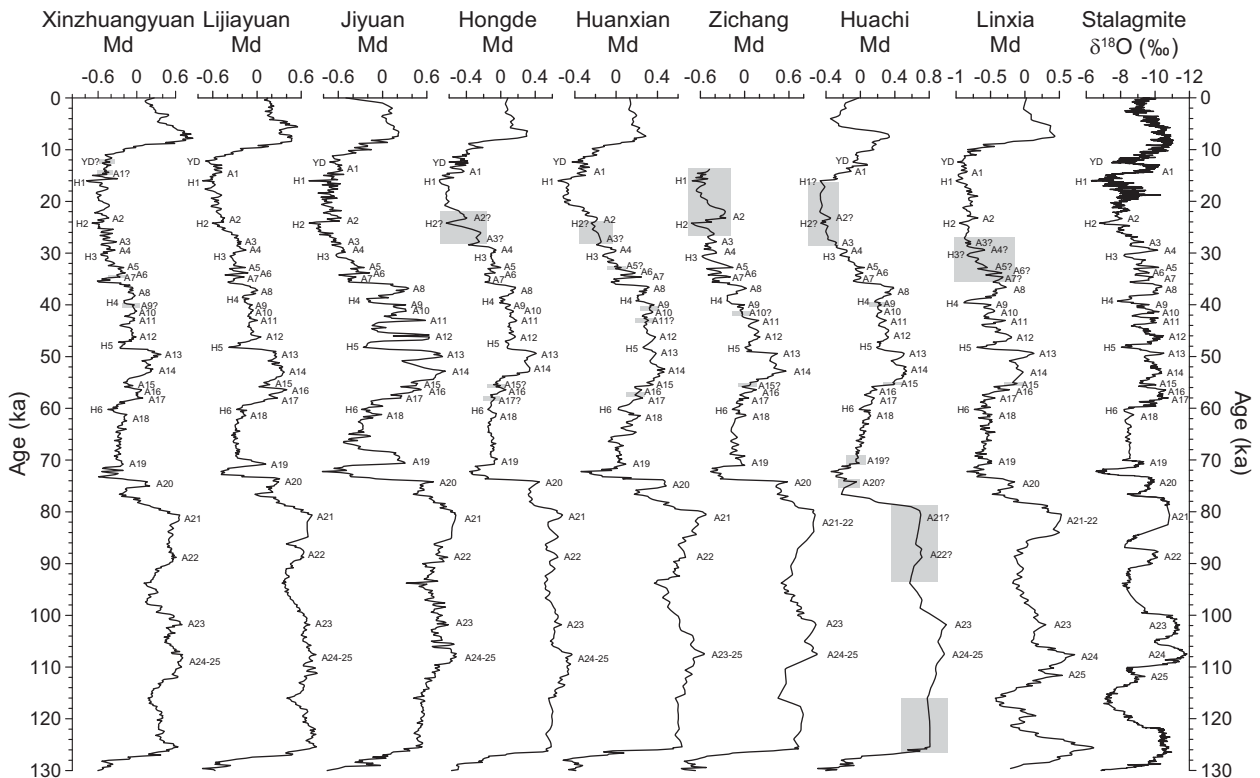


Figure 5. Correlation of the eight grain size records plotted on the stalagmite-based time scale for the interval 0–130 ka, and correlation with the stalagmite $\delta^{18}\text{O}$ record [Wang et al., 2008; Cheng et al., 2012]. Each grain size time series is normalized to an interval ranging from -1 to 1 . The Chinese Loess Interstadial (CLIS) events (A1–A25) are identified, following the nomenclature used in the stalagmite record [Cheng et al., 2006; Wang et al., 2008]. The Younger Dryas (YD) and Heinrich (H) events are also identified. The millennial-scale events possibly disturbed by depositional hiatuses are marked with “?”. The shaded areas indicate the parts that were excluded from the construction of the stacked grain size record shown in Figures 7–9.

to have been an extremely cold stadial. A recent study [Svendsen et al., 2004] has shown that a huge ice sheet complex formed over northern Eurasia during the late MIS 6 (the Late Saalian), which was one of the most extensive Quaternary glaciations in this part of the world. Since the accumulation of dust in China is closely related to the development of continental ice sheets in the Northern Hemisphere [Ding et al., 1995], the CHILOMOS record further implies that a large ice sheet should also have existed in Eurasia during MIS 7d, which requires investigation in future studies.

4.4. General Climatic Characteristics of the Last 249 kyr

As shown in the loess grain size record (Figure 9), millennial-scale events occurred frequently in the Loess Plateau during the last and penultimate glacials, and also took place in the last and penultimate interglacial complexes, but at a relatively low frequency. In general, Chinese loess records most of the millennial-scale events registered in Greenland ice and in Chinese stalagmites. From MIS 7 to 6, as well as from MIS 5 to 2, the millennial-scale oscillations were generally superimposed on a progressive cooling and drying trend, which culminated shortly prior to the termination (Figure 9). This pattern is not evident in the stalagmite record but is prominent in the benthic $\delta^{18}\text{O}$ record (Figure 9). As the benthic $\delta^{18}\text{O}$ record may primarily reflect the high northern-latitude ice volume, the loess deposits in northern China thus document climatic signals largely from the northern high-latitude ice sheets, while the stalagmites in southern China are more likely to mainly record signals from low latitudes.

5. Mechanisms

5.1. Trigger for Millennial-Scale Events

Since the identification of abrupt climatic changes in the last glaciation in Greenland [Dansgaard et al., 1993; Grootes et al., 1993], it has been found that such climatic events were pervasive globally in earlier glacial periods [Raymo et al., 1998; Ding et al., 1999; McManus et al., 1999; Voelker and Workshop Participants,

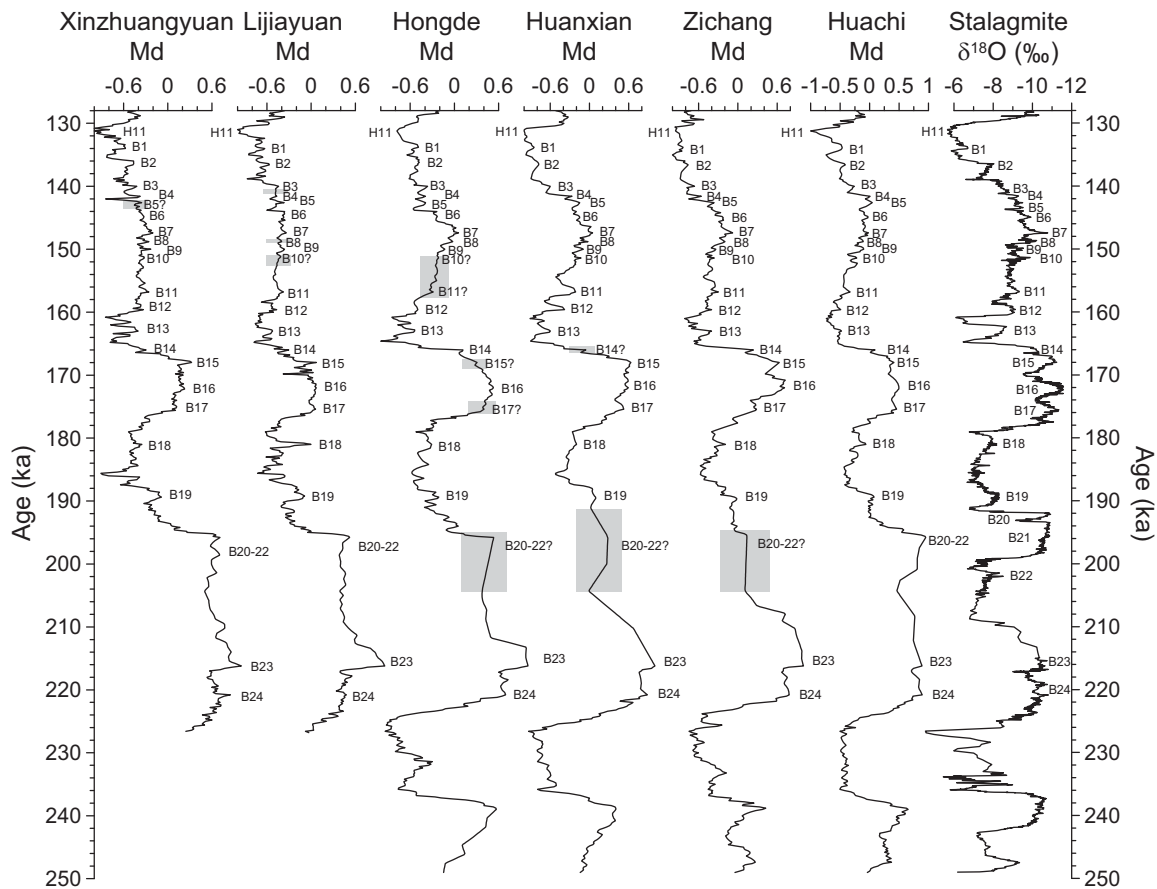


Figure 6. Correlation of the Xinzhuangyuan, Lijiayuan, Hongde, Huanxian, Zichang, and Huachi grain size records plotted on the stalagmite-based time scale for the interval 130–249 ka, and correlation with the stalagmite $\delta^{18}\text{O}$ record [Wang et al., 2008; Cheng et al., 2012]. Each grain size time series is normalized to an interval ranging from -1 to 1 . The Chinese Loess Interstadial (CLIS) events (B1–B24) are identified, following the nomenclature used in the stalagmite record [Cheng et al., 2006; Wang et al., 2008]. The H11 event is also identified. The millennial-scale events possibly disturbed by depositional hiatuses are marked with “?”. The shaded areas indicate the parts that were excluded from the construction of the stacked grain size record shown in Figures 8 and 9.

2002; Jouzel et al., 2007; Clement and Peterson, 2008]. As reviewed by Clement and Peterson [2008], the trigger for abrupt climate change may come from either low latitudes or high latitudes. The former notion suggests that changes in sea surface temperature (SST) in the tropical Pacific (e.g., El Niño-Southern Oscillation (ENSO)) may trigger abrupt climatic changes via ocean-atmosphere processes [Cane, 1998; Clement et al., 2001]. High-latitude forcing is mainly explained by two hypotheses: the sea ice [Gildor and Tziperman, 2003; Kaspi et al., 2004; Li et al., 2005; Wunsch, 2006] and the thermohaline circulation [Rooth, 1982; Broecker et al., 1985, 1990; Knutti et al., 2004] hypotheses. The former hypothesis states that sea ice in the Northern Hemisphere may drive abrupt climatic changes via its influence on albedo and the exchange of heat and moisture between ocean and atmosphere. The thermohaline circulation hypothesis is the currently preferred theory to explain abrupt climatic changes. It holds that the freshwater discharge into the North Atlantic leads to a reduction in the meridional overturning circulation (MOC), resulting in decreased oceanic heat transport from the Southern Ocean to the North Atlantic, and concomitant cooling in Greenland and warming in Antarctica. The MOC recovers when the freshwater perturbation stops, and the increased oceanic heat transport thus results in warming in Greenland and cooling in Antarctica. This process has come to be known as the bipolar seesaw and is evidenced by the ice-core records from Greenland and Antarctica (Figures 7 and 9) [Crowley, 1992; Stocker et al., 1992; Broecker, 1998; Stocker, 1998; Stocker and Johnsen, 2003; Knutti et al., 2004].

In D-O cycles, the temperature shifts in Greenland are as high as $8\text{--}16^\circ\text{C}$ [Lang et al., 1999; Landais et al., 2004; Huber et al., 2006], far greater than the values ($1\text{--}1.5^\circ\text{C}$) in the South China Sea [Zhao et al., 2006]

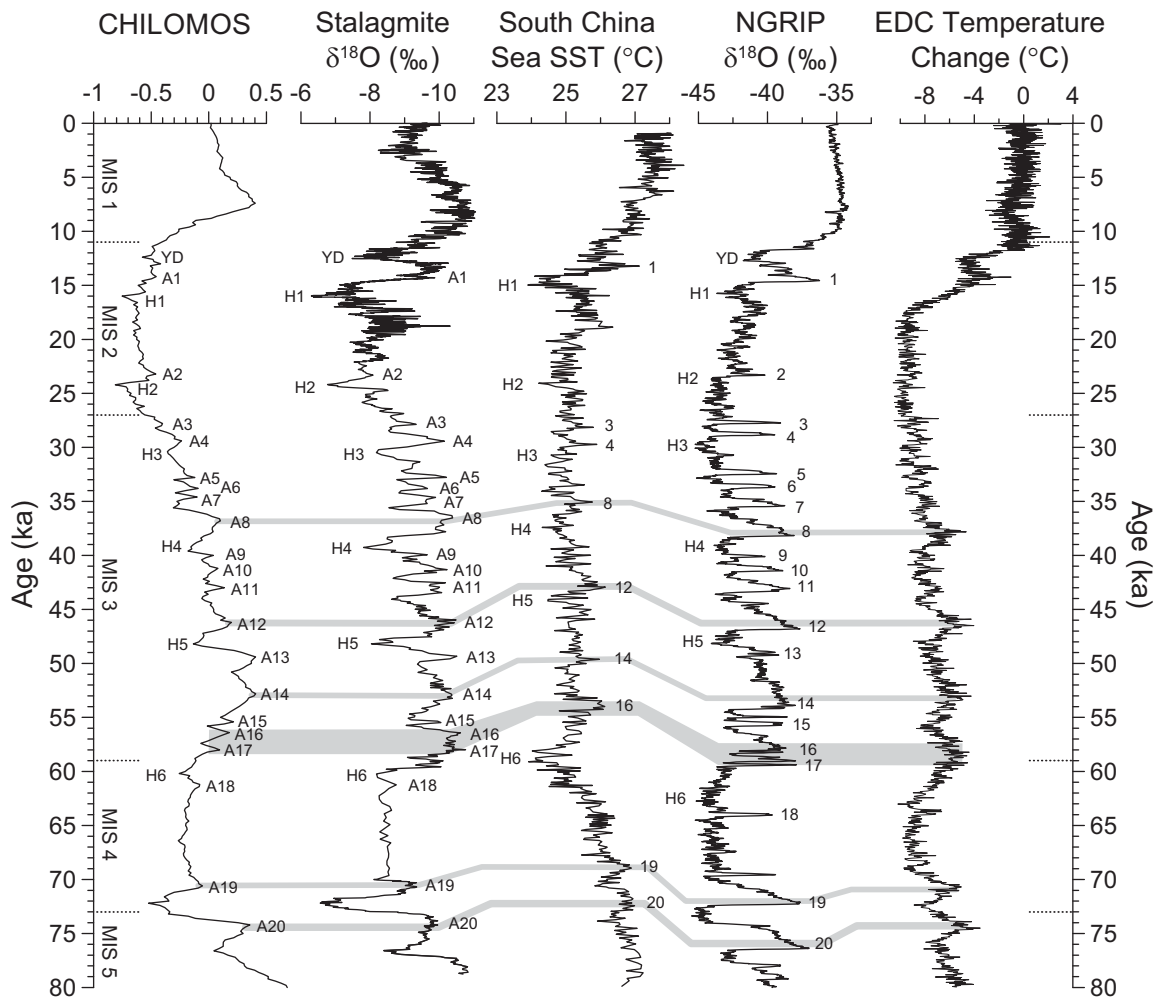


Figure 7. Millennial-scale events documented in the stacked grain size record of Chinese loess (CHILOMOS) for the last glacial period, and correlation with the stalagmite $\delta^{18}\text{O}$ record [Wang et al., 2008; Cheng et al., 2012], the sea surface temperature (SST) of the South China Sea [Zhao et al., 2006], the combined NGRIP $\delta^{18}\text{O}$ record from Greenland (five point smoothed) [North Greenland Ice Core Project Members, 2004; Svensson et al., 2008], and the EPICA Dome C (EDC) temperature anomaly in Antarctica [Jouzel et al., 2007]. The shaded bars indicate major interstadials. Marine isotope stages (MIS) are indicated.

(Figure 7) and the Sulu Sea [Dannenmann et al., 2003], and greater than the values (1–3°C) in Antarctica (Figure 7) [Watanabe et al., 2003; EPICA Community Members, 2006; Jouzel et al., 2007]. In addition, the longest D-O events in Greenland are strongly coupled with the largest warm events in the Loess Plateau, the South China Sea, and Antarctica (Figure 7). All these pieces of evidence show that the trigger for abrupt climate change originates in the northern polar area, as evidenced by the damped temperature oscillations from northern high latitudes to low latitudes. It is possible that slight changes in the SST of the tropical Pacific may have a large impact on the temperature in the northern polar area via amplifying mechanisms of ocean-atmosphere processes [e.g., Yin and Battisti, 2001; Ivanochko et al., 2005]. However, these physical processes remain to be identified, due to a lack of sufficient paleodata for SST from the tropics.

5.2. Propagation of Climatic Signals From Northern High Latitudes

Theoretically, the climatic signals of high northern latitudes could be propagated into the Loess Plateau through the influence of the North Atlantic, atmospheric CO_2 concentration, and latitudinal atmospheric circulation. These are discussed in detail in the following section.

5.2.1. North Atlantic

The ocean heat-conveyor belt may transmit high-latitude signals into the North Pacific, which then influences the East Asian summer monsoon. Oceanic ^{14}C data have shown that this propagation process may take

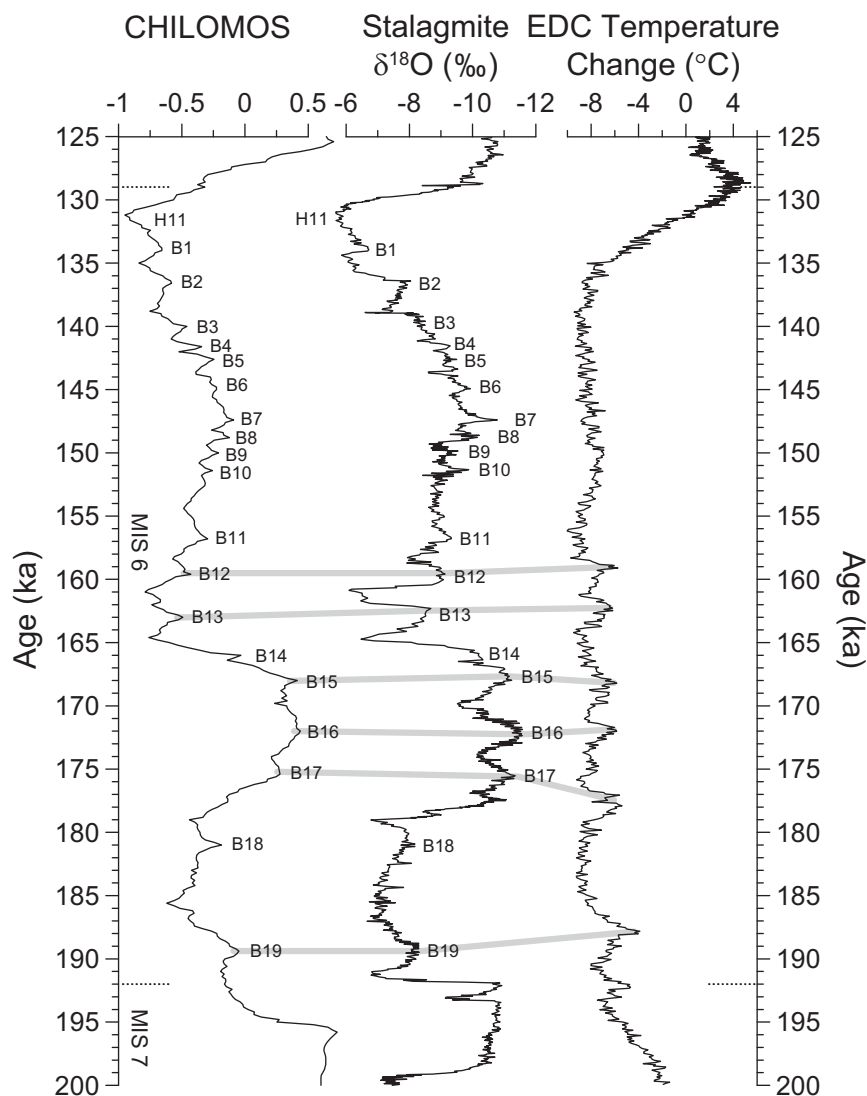


Figure 8. Millennial-scale events documented in the stacked grain size record of Chinese loess (CHILOMOS) for the penultimate glacial period, and correlation with the stalagmite $\delta^{18}\text{O}$ record [Wang *et al.*, 2008; Cheng *et al.*, 2012] and the EPICA Dome C (EDC) temperature anomaly in Antarctica [Jouzel *et al.*, 2007]. The shaded bars indicate major interstadials. Marine isotope stages (MIS) are indicated.

~1000 years [Matsumoto, 2007]. In this case, the D-O events registered in Chinese stalagmites should lag behind their Greenland counterparts. Given that the time scale for Greenland ice cores back to 14.5 ka is robust (as derived by counting annual layers), Wang *et al.* [2001] found a good synchronicity between Greenland ice cores and precisely dated Chinese stalagmites for the YD and D-O 1 (Bølling-Allerød) events. In addition, a recent study has shown highly synchronous (within ~20 years) changes in dust flux from Asian deserts and Greenland isotope records for abrupt climatic events [Steffensen *et al.*, 2008]. These pieces of evidence strongly suggest a synchronous change for D-O cycles between high northern latitudes and middle latitudes. This synchronicity for millennial-scale events seems to be common in the Northern Hemisphere [e.g., Hendy *et al.*, 2002; Lea *et al.*, 2003; Denniston *et al.*, 2007] and thus is unlikely to be explained in terms of thermohaline circulation changes.

The heat and moisture changes in the North Atlantic can also be transmitted to the Loess Plateau via the westerlies. On the one hand, high northern-latitude cooling can result in a southward shift of the westerlies, leading to an increase in moisture transport from the North Atlantic to East Asia. On the other hand, decreased SST can lead to weakened oceanic evaporation, thereby reducing the moisture transport. To evaluate the effect of the westerlies on precipitation in East Asia, rainfall data were collected from 11

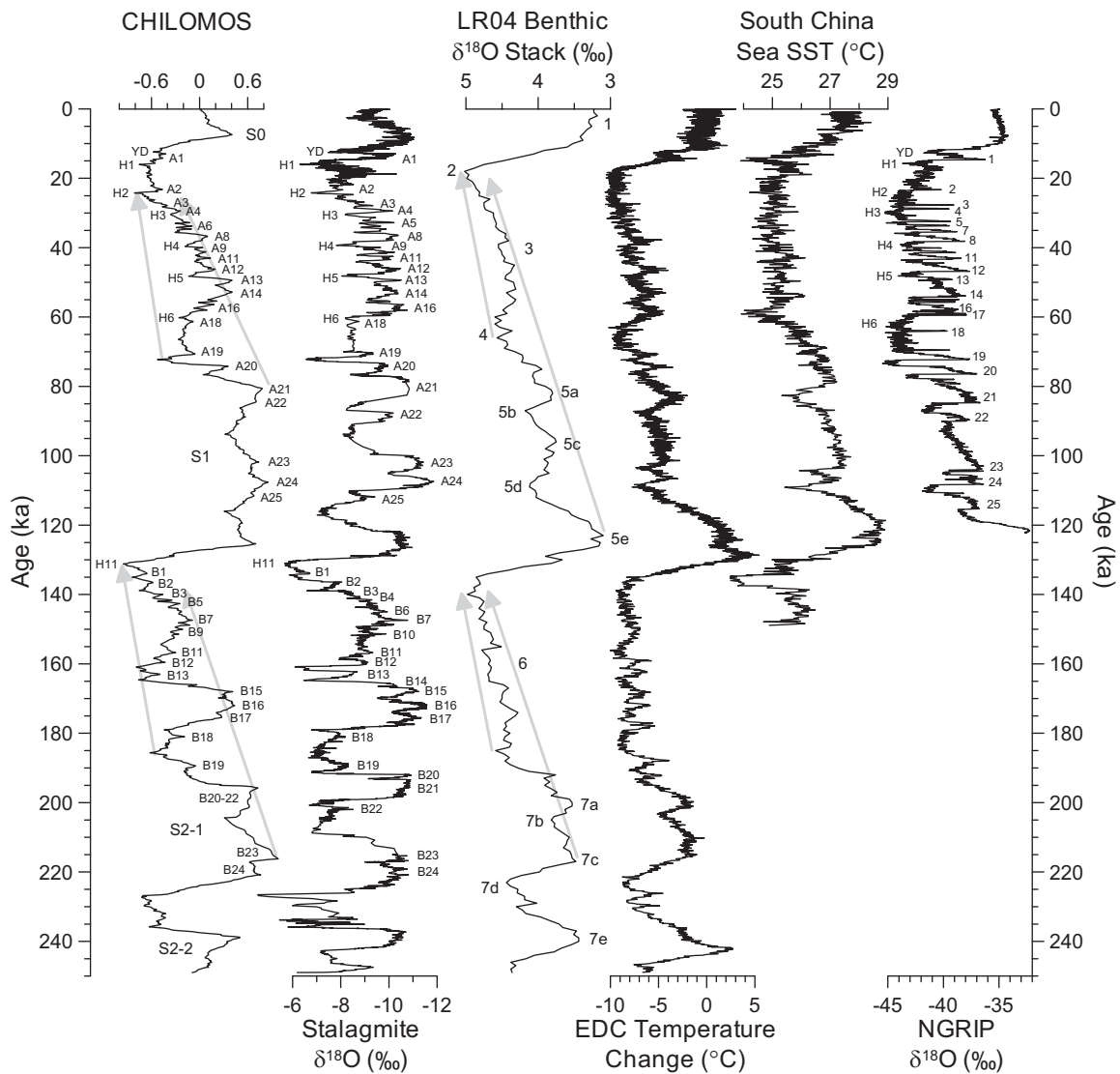


Figure 9. Millennial-scale events documented in the stacked grain size record of Chinese loess (CHILOMOS) for the last 249 kyr, and correlation with the stalagmite $\delta^{18}\text{O}$ record [Wang et al., 2008; Cheng et al., 2012], the LR04 benthic $\delta^{18}\text{O}$ stack [Lisiecki and Raymo, 2005], the EPICA Dome C temperature anomaly in Antarctica [Jouzel et al., 2007], the sea surface temperature (SST) of the South China Sea [Zhao et al., 2006], and the combined NGRIP $\delta^{18}\text{O}$ record from Greenland (five point smoothed) [North Greenland Ice Core Project Members, 2004; Svensson et al., 2008]. The shaded arrows indicate the long-term trend of the CHILOMOS and benthic $\delta^{18}\text{O}$ records in each glacial-interglacial cycle.

weather stations along a northwest-southeast transect running from the westerlies-dominated area [Tian et al., 2007; Pang et al., 2011] to the monsoon-dominated area (Figure 10). From northwest to southeast along the transect, the mean annual rainfall decreases gradually from Wulumuqi to Hami, then increases gradually from Anxi to Luochuan. This “V”-shape pattern clearly indicates that the Hami-Anxi area, with a mean annual rainfall below 50 mm, is at the easternmost limit of effective westerlies moisture and is likewise at the westernmost limit of effective summer monsoon moisture. In addition, it is physically implausible that the westerlies remain moisture-laden when reaching the Loess Plateau after a long voyage traversing the vast arid regions of central Asia (Figure 10). Therefore, the westerlies-related mechanism seems rather unlikely.

5.2.2. Atmospheric CO₂

Ice-core records have shown that atmospheric CO₂ variations were up to only 20 ppmv during the last glaciation, with the increase in CO₂ concentration occurring during the prominent cold periods (mainly Heinrich

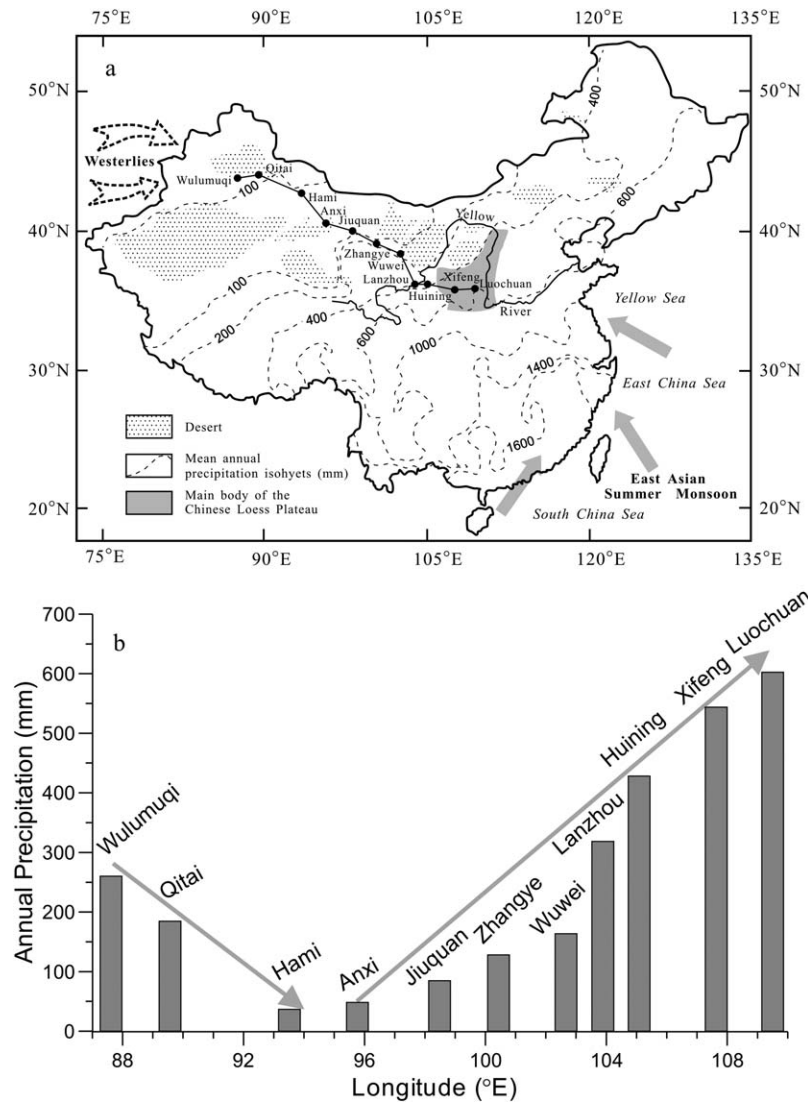


Figure 10. (a) Map showing the distribution of loess, desert, and mean annual precipitation isohyets (mm, dashed lines) in mainland China. The dashed and shaded arrows indicate the westerlies and East Asian summer monsoon winds, respectively. The 11 weather stations (solid circles) mark out a northwest-southeast transect running from the westerlies-dominated area [Tian et al., 2007; Pang et al., 2011] to the monsoon-dominated area. (b) Mean annual precipitation (mm) for the 11 sites along the transect. The shaded arrows indicate the spatial trend in annual rainfall changes.

events) of the Northern Hemisphere [Indermühle et al., 2000; Ahn and Brook, 2008]. According to Anderson et al. [2009], the intense high northern-latitude cooling induced a reorganization of global atmospheric circulation, leading to a southward shift of Southern Hemisphere westerlies and increased upwelling in the Southern Ocean. This upwelling would have raised CO₂-rich deep water to the surface and led to the rise in atmospheric CO₂ levels. It therefore follows that the variation in CO₂ is a result of climatic oscillations in the high northern latitudes, rather than a trigger for them.

5.2.3. Latitudinal Atmospheric Circulation

The East Asian winter monsoon is an interhemispheric circulation driven by the Siberian High [Chen et al., 1991; Webster et al., 1998; Wang et al., 2003]. The cold air accumulation in the Siberian region comes mainly from the Barents Sea, the Kara Sea, and the North Atlantic Ocean [Lydolph, 1977; Chen et al., 1991]. During glacial periods, these cold air source regions were either covered or greatly influenced by ice sheets [Imbrie et al., 1993; Lambeck, 1995]. It has been demonstrated that the strength of the winter monsoon is closely related to changes in ice volume in northern high latitudes [Ding et al., 1995]. The expansion of

high-latitude ice sheets was accompanied by a reduction in vegetation cover in middle latitudes and an increase in the albedo of the continental surface, which would thermally enhance the Siberian High. The expansion of ice sheets would also dynamically enhance the Siberian High by pushing more cold air masses to the middle latitudes. The combined thermal and dynamical effects of ice sheets would lead the Siberian High to persist longer in the annual cycle, thereby impeding the northward movement of moisture-laden monsoon airflows. Furthermore, the intensified northerly winter monsoon winds would impose a downstream cooling on the low-latitude oceans, particularly in the Western Pacific marginal seas, leading to weakened oceanic evaporation and a decreased summer monsoon season via a delayed onset. Clearly, temperature changes in the northern polar area could have played a significant role in millennial-scale variability in aridity over northern China through atmospheric forcing.

Some authors [Ding *et al.*, 1998] have proposed that the millennial-scale climatic signals might first have been transmitted into the Siberian High via the Barents and Kara Sea ice sheets, and then propagated into the Loess Plateau via the winter monsoon system. It has also been found that the millennial-scale variability in SST (Figure 7) and the productivity of the South China Sea are mainly controlled by the winter monsoons [Huang *et al.*, 1997; Wang *et al.*, 1999; Zhao *et al.*, 2006]. The synchronicity of millennial-scale climate events between Greenland and East Asia, as mentioned earlier, requires a rapid signal transmission, which is more likely to be associated with the monsoon circulation than with thermohaline processes. This monsoon-related mechanism, although it has been proposed in earlier studies [Ding *et al.*, 1998; Rohling *et al.*, 2003], merits systematic study in future work, particularly through paleoclimate modeling.

6. Discussion and Conclusions

Using correlation between sites of eight high-resolution grain size records from Chinese loess, and through the use of the Chinese stalagmite time scale, we constructed a stacked 249 kyr-long grain size time series of millennial-scale variability for the Chinese Loess Plateau (termed the "CHILOMOS" record). This stack documents most of the millennial-scale climatic events registered in Greenland and in Chinese stalagmites, and provides a common time scale and a comparative reference for millennial-scale records of Chinese loess, and will facilitate correlation of climate records from different archives. Correlations of climate records from high and low latitudes show that the millennial-scale abrupt changes originated in the northern polar area and were propagated into East Asia largely through the East Asian winter monsoon.

The CHILOMOS grain size record shows that the millennial-scale climatic events were superimposed on a prominent long-term cooling trend during both the last and penultimate glaciations, consistent with the pattern of increasing global ice volume (Figure 9). However, this cooling trend is dampened in the stalagmite record and is totally suppressed in the SST record of the South China Sea (Figure 9). These results lead us to the conclusion that the Loess Plateau of northern China is to a large extent influenced by the high-latitude ice sheets thanks to its great distance from the low-latitude ocean, while the proximal stalagmites of southern China are more reflective of signals from the low-latitude ocean. In this context, only when more Asian monsoon records from different latitudes become available can a clear picture of monsoon variability be developed.

The CHILOMOS record confirms that the driest and coldest interval of the last 249 kyr occurred in the late MIS 6. It also shows that MIS 7d, following an interglacial period lasting ~10 kyr (MIS 7e), was extremely cold and dry, similar to the climatic conditions of the stadials in MIS 6. This pervasive cold event within an interglacial complex was ascribed to the extreme summer insolation minima and large ice volume in the Northern Hemisphere [Ruddiman and McIntyre, 1982]. However, its spatial pattern and its causes require further study, given their importance for a better understanding of how and when the current interglacial will end, and given that humans are living in an interglacial period that has already lasted 12 kyr.

References

- Ahn, J., and E. J. Brook (2008), Atmospheric CO₂ and climate on millennial time scales during the last glacial period, *Science*, 322, 83–85, doi:10.1126/science.1160832.
- An, Z. S., G. Kukla, S. C. Porter, and J. L. Xiao (1991), Late Quaternary dust flow on the Chinese Loess Plateau, *Catena*, 18, 125–132, doi:10.1016/0341-8162(91)90012-M.
- Anderson, R. F., S. Ali, L. I. Bradtmiller, S. H. H. Nielsen, M. Q. Fleisher, B. E. Anderson, and L. H. Burckle (2009), Wind-driven upwelling in the Southern Ocean and the deglacial rise in atmospheric CO₂, *Science*, 323, 1443–1448, doi:10.1126/science.1167441.

Acknowledgments

This study was supported by the Strategic Priority Research Program of the Chinese Academy of Sciences (grants XDB03020503 and XDA05120204), and the National Basic Research Program of China (973 Program) (grant 2010CB950204). We thank Zhiwei Yu for help with grain size data processing, Bin Zhou, Jianzhang Ren, Xu Wang, Shengshan Hou, and Jimin Sun for field assistance, Zihua Tang and Zuoling Chen for discussions, and Meixun Zhao for providing the SST data. We are grateful to Edward Derbyshire and an anonymous reviewer for their constructive comments and to Louis Derry for editorial handling.

- Bond, G., W. Broecker, S. Johnsen, J. McManus, L. Labeyrie, J. Jouzel, and G. Bonani (1993), Correlations between climate records from North Atlantic sediments and Greenland ice, *Nature*, *365*, 143–147, doi:10.1038/365143a0.
- Broecker, W. S. (1998), Paleocirculation during the last deglaciation: A bipolar seesaw?, *Paleoceanography*, *13*, 119–121, doi:10.1029/97PA03707.
- Broecker, W. S., D. M. Peteet, and D. Rind (1985), Does the ocean-atmosphere system have more than one stable mode of operation?, *Nature*, *315*, 21–26, doi:10.1038/315021a0.
- Broecker, W. S., G. Bond, M. Klas, G. Bonani, and W. Wolfi (1990), A salt oscillator in the glacial Atlantic? 1. The concept, *Paleoceanography*, *5*, 469–477, doi:10.1029/PA005i004p00469.
- Cane, M. A. (1998), A role for the tropical Pacific, *Science*, *282*, 59–61, doi:10.1126/science.282.5386.59.
- Chen, L. X., Q. G. Zhu, H. B. Luo, J. H. He, M. Dong, and Z. Q. Feng (1991), *The East-Asian Monsoon* [in Chinese], China Meteorol. Press, Beijing.
- Chen, F. H., J. Bloemendal, J. M. Wang, J. J. Li, and F. Oldfield (1997), High-resolution multi-proxy climate records from Chinese loess: Evidence for rapid climatic changes over the last 75 kyr, *Palaeogeogr. Palaeoclimatol. Palaeoecol.*, *130*, 323–335, doi:10.1016/S0031-0182(96)00149-6.
- Chen, F. H., J. Bloemendal, Z. D. Feng, J. M. Wang, E. Parker, and Z. T. Guo (1999), East Asian monsoon variations during Oxygen Isotope Stage 5: Evidence from the northwestern margin of the Chinese loess plateau, *Quat. Sci. Rev.*, *18*, 1127–1135, doi:10.1016/S0277-3791(98)00047-X.
- Cheng, H., R. L. Edwards, Y. Wang, X. Kong, Y. Ming, M. J. Kelly, X. Wang, C. D. Gallup, and W. Liu (2006), A penultimate glacial monsoon record from Hulu Cave and two-phase glacial terminations, *Geology*, *34*, 217–220, doi:10.1130/G22289.1.
- Cheng, H., P. Z. Zhang, C. Spötl, R. L. Edwards, Y. J. Cai, D. Z. Zhang, W. C. Sang, M. Tan, and Z. S. An (2012), The climatic cyclicity in semiarid-arid central Asia over the past 500,000 years, *Geophys. Res. Lett.*, *39*, L01705, doi:10.1029/2011GL050202.
- Clement, A. C., and L. C. Peterson (2008), Mechanisms of abrupt climate change of the last glacial period, *Rev. Geophys.*, *46*, RG4002, doi:10.1029/2006RG000204.
- Clement, A. C., M. A. Cane, and R. Seager (2001), An orbitally driven tropical source for abrupt climate change, *J. Clim.*, *14*, 2369–2375, doi:10.1175/1520-0442(2001)014<2369:AODTSF>2.0.CO;2.
- Crowley, T. J. (1992), North Atlantic deep water cools the Southern Hemisphere, *Paleoceanography*, *7*, 489–497, doi:10.1029/92PA01058.
- Dannenmann, S., B. K. Linsley, D. W. Oppo, Y. Rosenthal, and L. Beaufort (2003), East Asian monsoon forcing of suborbital variability in the Sulu Sea during Marine Isotope Stage 3: Link to Northern Hemisphere climate, *Geochem. Geophys. Geosyst.*, *4*(1), 1001, doi:10.1029/2002GC000390.
- Dansgaard, W., et al. (1993), Evidence for general instability of past climate from a 250-kyr ice-core record, *Nature*, *364*, 218–220, doi:10.1038/364218a0.
- Denniston, R. F., Y. Asmerom, V. Polyak, J. A. Dorale, S. J. Carpenter, C. Trodick, B. Hoyer, and L. A. González (2007), Synchronous millennial-scale climatic changes in the Great Basin and the North Atlantic during the last interglacial, *Geology*, *35*, 619–622, doi:10.1130/G23445A.1.
- Ding, Z., Z. Yu, N. W. Rutter, and T. Liu (1994), Towards an orbital time scale for Chinese loess deposits, *Quat. Sci. Rev.*, *13*, 39–70, doi:10.1016/0277-3791(94)90124-4.
- Ding, Z., T. Liu, N. W. Rutter, Z. Yu, Z. Guo, and R. Zhu (1995), Ice-volume forcing of East Asian winter monsoon variations in the past 800,000 years, *Quat. Res.*, *44*, 149–159, doi:10.1006/qres.1995.1059.
- Ding, Z. L., N. W. Rutter, T. S. Liu, J. M. Sun, J. Z. Ren, D. Rokosh, and S. F. Xiong (1998), Correlation of Dansgaard-Oeschger cycles between Greenland ice and Chinese loess, *Paleoclimates*, *2*, 281–291.
- Ding, Z. L., J. Z. Ren, S. L. Yang, and T. S. Liu (1999), Climate instability during the penultimate glaciation: Evidence from two high-resolution loess records, China, *J. Geophys. Res.*, *104*, 20,123–20,132, doi:10.1029/1999JB900183.
- Ding, Z. L., E. Derbyshire, S. L. Yang, Z. W. Yu, S. F. Xiong, and T. S. Liu (2002), Stacked 2.6-Ma grain size record from the Chinese loess based on five sections and correlation with the deep-sea $\delta^{18}\text{O}$ record, *Paleoceanography*, *17*(3), 1033, doi:10.1029/2001PA000725.
- Ding, Z. L., E. Derbyshire, S. L. Yang, J. M. Sun, and T. S. Liu (2005), Stepwise expansion of desert environment across northern China in the past 3.5 Ma and implications for monsoon evolution, *Earth Planet. Sci. Lett.*, *237*, 45–55, doi:10.1016/j.epsl.2005.06.036.
- EPICA Community Members (2006), One-to-one coupling of glacial climate variability in Greenland and Antarctica, *Nature*, *444*, 195–198, doi:10.1038/nature05301.
- Fang, X. M., et al. (1999), Asian summer monsoon instability during the past 60,000 years: Magnetic susceptibility and pedogenic evidence from the western Chinese Loess Plateau, *Earth Planet. Sci. Lett.*, *168*, 219–232, doi:10.1016/S0012-821X(99)00053-9.
- Gildor, H., and E. Tziperman (2003), Sea-ice switches and abrupt climate change, *Philos. Trans. R. Soc. London A*, *361*, 1935–1944, doi:10.1098/rsta.2003.1244.
- Groote, P. M., M. Stuiver, J. W. C. White, S. Johnsen, and J. Jouzel (1993), Comparison of oxygen isotope records from the GISP2 and GRIP Greenland ice cores, *Nature*, *366*, 552–554, doi:10.1038/366552a0.
- Heinrich, H. (1988), Origin and consequences of cyclic ice rafting in the Northeast Atlantic Ocean during the past 130,000 years, *Quat. Res.*, *29*, 142–152, doi:10.1016/0033-5894(88)90057-9.
- Hendy, I. L., J. P. Kennett, E. B. Roark, and B. L. Ingram (2002), Apparent synchronicity of submillennial scale climate events between Greenland and Santa Barbara Basin, California from 30–10 ka, *Quat. Sci. Rev.*, *21*, 1167–1184, doi:10.1016/S0277-3791(01)00138-X.
- Huang, C. Y., S. F. Wu, M. Zhao, M. T. Chen, C. H. Wang, X. Tu, and P. B. Yuan (1997), Surface ocean and monsoon climate variability in the South China Sea since the last glaciation, *Mar. Micropaleontol.*, *32*, 71–94, doi:10.1016/S0377-8398(97)00014-5.
- Huber, C., M. Leuenberger, R. Spahni, J. Flückiger, J. Schwander, T. F. Stocker, S. Johnsen, A. Landais, and J. Jouzel (2006), Isotope calibrated Greenland temperature record over Marine Isotope Stage 3 and its relation to CH_4 , *Earth Planet. Sci. Lett.*, *243*, 504–519, doi:10.1016/j.epsl.2006.01.002.
- Imbrie, J., et al. (1993), On the structure and origin of major glaciation cycles 2. The 100,000-year cycle, *Paleoceanography*, *8*, 699–735, doi:10.1029/93PA02751.
- Indermühle, A., E. Monnin, B. Stauffer, T. F. Stocker, and M. Wahlen (2000), Atmospheric CO_2 concentration from 60 to 20 kyr BP from the Taylor Dome ice core, Antarctica, *Geophys. Res. Lett.*, *27*, 735–738, doi:10.1029/1999GL010960.
- Ivanochko, T. S., R. S. Ganeshram, G. J. A. Brummer, G. Ganssen, S. J. A. Jung, S. G. Moreton, and D. Kroon (2005), Variations in tropical convection as an amplifier of global climate change at the millennial scale, *Earth Planet. Sci. Lett.*, *235*, 302–314, doi:10.1016/j.epsl.2005.04.002.
- Jouzel, J., et al. (2007), Orbital and millennial Antarctic climate variability over the past 800,000 years, *Science*, *317*, 793–796, doi:10.1126/science.1141038.

- Kaspi, Y., R. Sayag, and E. Ziperman (2004), A "triple sea-ice state" mechanism for the abrupt warming and synchronous ice sheet collapses during Heinrich events, *Paleoceanography*, *19*, PA3004, doi:10.1029/2004PA001009.
- Knutti, R., J. Flückiger, T. F. Stocker, and A. Timmermann (2004), Strong hemispheric coupling of glacial climate through freshwater discharge and ocean circulation, *Nature*, *430*, 851–856, doi:10.1038/nature02786.
- Kukla, G. (1987), Loess stratigraphy in Central China, *Quat. Sci. Rev.*, *6*, 191–219, doi:10.1016/0277-3791(87)90004-7.
- Lambeck, K. (1995), Constraints on the Late Weichselian ice sheet over the Barents Sea from observations of raised shorelines, *Quat. Sci. Rev.*, *14*, 1–16, doi:10.1016/0277-3791(94)00107-M.
- Landais, A., N. Caillon, C. Goujon, A. M. Grachev, J. M. Barnola, J. Chappellaz, J. Jouzel, V. Masson-Delmotte, and M. Leuenberger (2004), Quantification of rapid temperature change during DO event 12 and phasing with methane inferred from air isotopic measurements, *Earth Planet. Sci. Lett.*, *225*, 221–232, doi:10.1016/j.epsl.2004.06.009.
- Lang, C., M. Leuenberger, J. Schwander, and S. Johnsen (1999), 16°C rapid temperature variation in Central Greenland 70,000 years ago, *Science*, *286*, 934–937, doi:10.1126/science.286.5441.934.
- Lea, D. W., D. K. Pak, L. C. Peterson, and K. A. Hughen (2003), Synchronicity of tropical and high-latitude Atlantic temperatures over the last glacial termination, *Science*, *301*, 1361–1364, doi:10.1126/science.1088470.
- Li, C., D. S. Battisti, D. P. Schrag, and E. Ziperman (2005), Abrupt climate shifts in Greenland due to displacements of the sea ice edge, *Geophys. Res. Lett.*, *32*, L19702, doi:10.1029/2005GL023492.
- Lisiecki, L. E., and M. E. Raymo (2005), A Pliocene-Pleistocene stack of 57 globally distributed benthic $\delta^{18}\text{O}$ records, *Paleoceanography*, *20*, PA1003, doi:10.1029/2004PA001071.
- Liu, T. S. (1985), *Loess and the Environment*, China Ocean Press, Beijing.
- Lu, H., K. O. van Huissteden, Z. An, G. Nugteren, and J. Vandenberghe (1999), East Asia winter monsoon variations on a millennial time-scale before the last glacial-interglacial cycle, *J. Quat. Sci.*, *14*, 101–110, doi:10.1002/(SICI)1099-1417(199903)14:2<101::AID-JQS433>3.0.CO;2-M.
- Lu, Y. C., X. L. Wang, and A. G. Wintle (2007), A new OSL chronology for dust accumulation in the last 130,000 yr for the Chinese Loess Plateau, *Quat. Res.*, *67*, 152–160, doi:10.1016/j.yqres.2006.08.003.
- Lydolph, P. E. (1977), *Climates of the Soviet Union*, Elsevier, Amsterdam.
- Matsumoto, K. (2007), Radiocarbon-based circulation age of the world oceans, *J. Geophys. Res.*, *112*, C09004, doi:10.1029/2007JC004095.
- McManus, J. F., D. W. Oppo, and J. L. Cullen (1999), A 0.5-million-year record of millennial-scale climate variability in the North Atlantic, *Science*, *283*, 971–975, doi:10.1126/science.283.5404.971.
- North Greenland Ice Core Project Members (2004), High-resolution record of Northern Hemisphere climate extending into the last interglacial period, *Nature*, *431*, 147–151, doi:10.1038/nature02805.
- Pang, Z., Y. Kong, K. Froehlich, T. Huang, L. Yuan, Z. Li, and F. Wang (2011), Processes affecting isotopes in precipitation of an arid region, *Tellus, Ser. B*, *63*, 352–359, doi:10.1111/j.1600-0889.2011.00532.x.
- Penaud, A., F. Eynaud, J. L. Turon, S. Zaragosi, F. Marret, and J. F. Bourillet (2008), Interglacial variability (MIS 5 and MIS 7) and dinoflagellate cyst assemblages in the Bay of Biscay (North Atlantic), *Mar. Micropaleontol.*, *68*, 136–155, doi:10.1016/j.marmicro.2008.01.007.
- Porter, S. C., and Z. S. An (1995), Correlation between climate events in the North Atlantic and China during the last glaciation, *Nature*, *375*, 305–308, doi:10.1038/375305a0.
- Prokopenko, A. A., E. B. Karabanov, D. F. Williams, M. I. Kuzmin, N. J. Shackleton, S. J. Crowhurst, J. A. Peck, A. N. Gvozdkov, and J. W. King (2001), Biogenic silica record of the Lake Baikal response to climatic forcing during the Brunhes, *Quat. Res.*, *55*, 123–132, doi:10.1006/qres.2000.2212.
- Raymo, M. E., K. Ganley, S. Carter, D. W. Oppo, and J. McManus (1998), Millennial-scale climate instability during the early Pleistocene epoch, *Nature*, *392*, 699–702, doi:10.1038/33658.
- Rohling, E. J., P. A. Mayewski, and P. Challenor (2003), On the timing and mechanism of millennial-scale climate variability during the last glacial cycle, *Clim. Dyn.*, *20*, 257–267, doi:10.1007/s00382-002-0266-4.
- Rooth, C. (1982), Hydrology and ocean circulation, *Prog. Oceanogr.*, *11*, 131–149, doi:10.1016/0079-6611(82)90006-4.
- Roucoux, K. H., P. C. Tzedakis, L. de Abreu, and N. J. Shackleton (2006), Climate and vegetation changes 180,000 to 345,000 years ago recorded in a deep-sea core off Portugal, *Earth Planet. Sci. Lett.*, *249*, 307–325, doi:10.1016/j.epsl.2006.07.005.
- Roucoux, K. H., P. C. Tzedakis, M. R. Frogley, I. T. Lawson, and R. C. Preece (2008), Vegetation history of the marine isotope stage 7 interglacial complex at Ioannina, NW Greece, *Quat. Sci. Rev.*, *27*, 1378–1395, doi:10.1016/j.quascirev.2008.04.002.
- Ruddiman, W. F., and A. McIntyre (1982), Severity and speed of Northern Hemisphere glaciation pulses: The limiting case?, *Geol. Soc. Am. Bull.*, *93*, 1273–1279, doi:10.1130/0016-7606(1982)93<1273:SASONH>2.0.CO;2.
- Steffensen, J. P., et al. (2008), High-resolution Greenland ice core data show abrupt climate change happens in few years, *Science*, *321*, 680–684, doi:10.1126/science.1157707.
- Stevens, T., S. J. Armitage, H. Lu, and D. S. G. Thomas (2006), Sedimentation and diagenesis of Chinese loess: Implications for the preservation of continuous, high-resolution climate records, *Geology*, *34*, 849–852, doi:10.1130/G22472.1.
- Stocker, T. F. (1998), The seesaw effect, *Science*, *282*, 61–62, doi:10.1126/science.282.5386.61.
- Stocker, T. F., and S. J. Johnsen (2003), A minimum thermodynamic model for the bipolar seesaw, *Paleoceanography*, *18*(4), 1087, doi:10.1029/2003PA000920.
- Stocker, T. F., D. G. Wright, and W. S. Broecker (1992), The influence of high-latitude surface forcing on the global thermohaline circulation, *Paleoceanography*, *7*, 529–541, doi:10.1029/92PA01695.
- Sun, Y., S. C. Clemens, C. Morrill, X. Lin, X. Wang, and Z. An (2012), Influence of Atlantic meridional overturning circulation on the East Asian winter monsoon, *Nat. Geosci.*, *5*, 46–49, doi:10.1038/NGEO1326.
- Svendsen, J. I., et al. (2004), Late Quaternary ice sheet history of northern Eurasia, *Quat. Sci. Rev.*, *23*, 1229–1271, doi:10.1016/j.quascirev.2003.12.008.
- Svensson, A., et al. (2008), A 60,000 year Greenland stratigraphic ice core chronology, *Clim. Past*, *4*, 47–57, doi:10.5194/cp-4-47-2008.
- Tian, L., T. Yao, K. MacClune, J. W. C. White, A. Schilla, B. Vaughn, R. Vachon, and K. Ichiyanagi (2007), Stable isotopic variations in west China: A consideration of moisture sources, *J. Geophys. Res.*, *112*, D10112, doi:10.1029/2006JD007718.
- Tzedakis, P. C., J. F. McManus, H. Hooghiemstra, D. W. Oppo, and T. A. Wijmstra (2003), Comparison of changes in vegetation in northeast Greece with records of climate variability on orbital and suborbital frequencies over the last 450,000 years, *Earth Planet. Sci. Lett.*, *212*, 197–212, doi:10.1016/S0012-821X(03)00233-4.
- Voelker, A. H. L., and Workshop Participants (2002), Global distribution of centennial-scale records for Marine Isotope Stage (MIS) 3: A database, *Quat. Sci. Rev.*, *21*, 1185–1212, doi:10.1016/S0277-3791(01)00139-1.

- Wang, L., et al. (1999), East Asian monsoon climate during the Late Pleistocene: High-resolution sediment records from the South China Sea, *Mar. Geol.*, *156*, 245–284, doi:10.1016/S0025-3227(98)00182-0.
- Wang, Y. J., H. Cheng, R. L. Edwards, Z. S. An, J. Y. Wu, C. C. Shen, and J. A. Dorale (2001), A high-resolution absolute-dated late Pleistocene monsoon record from Hulu Cave, China, *Science*, *294*, 2345–2348, doi:10.1126/science.1064618.
- Wang, B., S. C. Clemens, and P. Liu (2003), Contrasting the Indian and East Asian monsoons: Implications on geologic timescales, *Mar. Geol.*, *201*, 5–21, doi:10.1016/S0025-3227(03)00196-8.
- Wang, Y., et al. (2008), Millennial- and orbital-scale changes in the East Asian monsoon over the past 224,000 years, *Nature*, *451*, 1090–1093, doi:10.1038/nature06692.
- Watanabe, O., J. Jouzel, S. Johnsen, F. Parrenin, H. Shoji, and N. Yoshida (2003), Homogeneous climate variability across East Antarctica over the past three glacial cycles, *Nature*, *422*, 509–512, doi:10.1038/nature01525.
- Webster, P. J., V. O. Magaña, T. N. Palmer, J. Shukla, R. A. Tomas, M. Yanai, and T. Yasunari (1998), Monsoons: Processes, predictability, and the prospects for prediction, *J. Geophys. Res.*, *103*, 14,451–14,510, doi:10.1029/97JC02719.
- Wunsch, C. (2006), Abrupt climate change: An alternative view, *Quat. Res.*, *65*, 191–203, doi:10.1016/j.yqres.2005.10.006.
- Xiao, J. L., S. C. Porter, Z. S. An, H. Kumai, and S. Yoshikawa (1995), Grain size of quartz as an indicator of winter monsoon strength on the Loess Plateau of central China during the last 130,000 yr, *Quat. Res.*, *43*, 22–29, doi:10.1006/qres.1995.1003.
- Yang, S., and Z. Ding (2008), Advance-retreat history of the East-Asian summer monsoon rainfall belt over northern China during the last two glacial-interglacial cycles, *Earth Planet. Sci. Lett.*, *274*, 499–510, doi:10.1016/j.epsl.2008.08.001.
- Yang, S. L., and Z. L. Ding (2004), Comparison of particle size characteristics of the Tertiary 'red clay' and Pleistocene loess in the Chinese Loess Plateau: implications for origin and sources of the 'red clay,' *Sedimentology*, *51*, 77–93, doi:10.1046/j.1365-3091.2003.00612.x.
- Yin, J. H., and D. S. Battisti (2001), The importance of tropical sea surface temperature patterns in simulations of Last Glacial Maximum climate, *J. Clim.*, *14*, 565–581, doi:10.1175/1520-0442(2001)014<0565:TLOTSS>2.0.CO;2.
- Zhao, M., C. Y. Huang, C. C. Wang, and G. Wei (2006), A millennial-scale U_{37}^K sea-surface temperature record from the South China Sea (8°N) over the last 150 kyr: Monsoon and sea-level influence, *Palaeogeogr. Palaeoclimatol. Palaeoecol.*, *236*, 39–55, doi:10.1016/j.palaeo.2005.11.033.
- Zhu, R., R. Zhang, C. Deng, Y. Pan, Q. Liu, and Y. Sun (2007), Are Chinese loess deposits essentially continuous?, *Geophys. Res. Lett.*, *34*, L17306, doi:10.1029/2007GL030591.